Predictive Molecular Model for the Thermodynamic and Transport Properties of Triacylglycerols

Amadeu K. Sum, Mary J. Biddy, and Juan J. de Pablo*

Department of Chemical and Biological Engineering, University of Wisconsin, Madison, Wisconsin 53706

Michael J. Tupy

Cargill Inc., Process Solutions Technology Development Center, Minneapolis, Minnesota 55440

Received: July 2, 2003

A molecular model is presented for triacylglycerides. These molecules are the main constituent of natural oils, and they are being increasingly sought out for novel technological applications (e.g. in high-performance, biodegradable lubricants). The model is derived from a combination of quantum-mechanical calculations, molecular simulations, and comparisons to experiment. It is shown to be capable of describing a number of equilibrium thermodynamic and transport properties for pure triacylglycerides and their mixtures. Calculated densities and viscosities are in good agreement with available experimental data. Predictions of the viscosity of several multicomponent mixtures, such as canola oil, cocoa butter, and commercial-grade lubricants, also show good agreement with reported values. The proposed model is also used to explore relations between the structure and properties of different functionalities (e.g. position of ethyl branches along the main chain), thereby providing insights into how some chemical treatments might alter the physical properties of natural oils.

1. Introduction

It is now possible to predict the phase behavior and transport properties of alkanes and their mixtures with good accuracy. One of the basic questions addressed in this work is whether a simple force field originally derived for alkanes can be extended for applications involving triacylglycerols. Triacylglycerols, also known as triglycerides or simply TAGs, are the major component of naturally occurring oils and fats (e.g., cotton, sunflower, corn, soybean, and cocoa oil and butter fat). They are abundant and biodegradable.[1−9]

One promising application that has emerged in recent years is their use as the basis for environmentally benign lubricants. However, the thermodynamic and transport properties of triglycerides in their natural form are not optimal for lubrication applications; chemical modifications are necessary to improve such properties. The number of alterations that can be made are boundless, and the design of triglycerides with specific lubrication properties would benefit considerably from theoretical models capable of predicting viscosities and thermodynamic properties from knowledge of molecular structures and composition.

Triglycerides can be formed from the condensation reaction of glycerol and fatty acids,[10,11] as illustrated in Figure 1. The fatty acids can vary widely in structure and functionality. For naturally occurring oils, these consist of long aliphatic chains (straight chain alkanes and alkenes). The three chains can be identical or can vary in length, structure, and functionality. Some of the most common triglycerides are formed from lauric acid (L), palmitic acid (P), stearic acid (S), oleic acid (O), linoleic acid (Li), and linolenic acid (Le). In naturally occurring oils, the fatty acids tend to have an even number of carbons, usually between 16 and 20. A commonly used nomenclature scheme for triglycerides is based on the functionality and length of the constituent fatty acids. For example, tripalmitin is made from three palmitic acids, and triolein from three oleic acids. Triglycerides are also often identified by a three-letter acronym representing the respective fatty acids and their order in the molecule. Thus, tripalmitin can also be denoted by PPP, triolein by OOO, and a mixed triglyceride composed of two stearic acids at the ends and one linoleic acid in the middle position by SLiS.

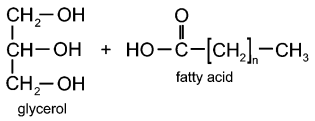

Figure 1. Condensation reaction for the formation of triacylglycerols.

To our knowledge, most computational studies of triglycerides have been focused on their crystal structure.[12−15] Isolated molecules in a vacuum have been examined using molecular mechanics,[16] and a single LLL molecule in dilute aqueous solution has also been considered.[17] There are no reported molecular studies of triglycerides in the liquid form, which is the state most relevant for lubrication applications.

In this work we present a force field capable of describing the density and heat of vaporization of triglycerides. It is also capable of describing its viscosity. Results are reported for both pure components and several mixtures of practical significance and for a wide variety of molecules.

2. Force Field Development

The approach adopted in this work relies to a significant extent on information generated by means of quantum-chemical calculations. The current tools of quantum chemistry permit

* To whom correspondence should be addressed. E-mail: depablo@engr.wisc.edu.

10.1021/jp035906g CCC: $25.00
Published on Web 12/02/2003

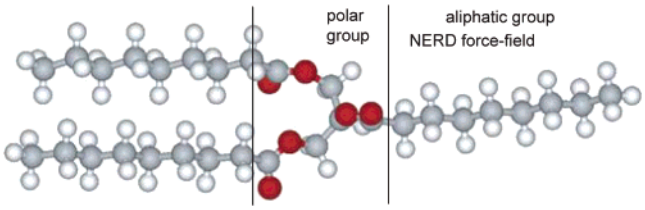

Figure 2. Sample triglyceride molecule. The molecule can be separated into two groups: a polar part containing the glycerol backbone and an aliphatic part composing each of the chains.

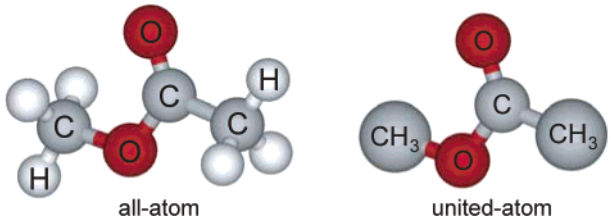

Figure 3. Methyl acetate molecule used as a model for the polar group of the triglyceride.

detailed studies of the most important modes of interactions usually employed in simulations, that is, intra- and intermolecular modes of interaction. Intramolecular interactions include bond vibration, bond bending, and torsion potentials. Triglycerides are fairly large molecules, often comprised of 50−70 heavy atoms; to render our electronic structure calculations more tractable, we chose to divide the triglyceride into two parts: a polar headgroup, including the glycerol backbone and ester linkage, and the aliphatic chains (see Figure 2).

A number of force fields are available for generic organic compounds, such as CHARMM,[18] AMBER,[19,20] and OPLS.[21] In this work we adopt the NERD force field,[22−24] a united-atom model (methyl or methylene groups are represented by a single interaction site) that has proven to accurately predict the thermophysical properties of a variety of straight chain and branched alkanes as well as alkenes. This force field is used to describe the aliphatic part of the triglycerides; it is given by

$$U^{\text{total}} = U^{\text{inter}} + U^{\text{intra}} \tag{1}$$

$$U^{\text{inter}} = U^{\text{LJ}} = \sum_{i>j} 4\epsilon_{ij}\left[\left(\frac{\sigma_{ij}}{r_{ij}}\right)^{12} - \left(\frac{\sigma_{ij}}{r_{ij}}\right)^{6}\right] \tag{2}$$

$$U^{\text{intra}} = U^{\text{bond}} + U^{\text{angle}} + U^{\text{torsion}} \tag{3}$$

$$U^{\text{bond}} = \sum_{\text{all bonds}} \frac{K_r}{2}(r - r_{\text{eq}})^2 \tag{4}$$

$$U^{\text{angle}} = \sum_{\text{all angles}} \frac{K_\theta}{2}(\theta - \theta_{\text{eq}})^2 \tag{5}$$

$$U^{\text{torsion}} = \sum_{\text{all torsions}} \sum_{n} \frac{V_n}{2}[1 - \cos n(\phi - \phi_{\text{eq}})] \tag{6}$$

where ϵ and σ are Lennard-Jones parameters for interactions between sites i and j (based on the Lorentz−Berthelot combining rule[25]), r_{ij} is the distance between sites i and j, K_r and K_θ are the force constants for the bond stretching and bond bending potentials, respectively, θ is the angle between adjacent bonds, V_n are the Fourier coefficients for the torsion potential, and ϕ is the torsion angle. In the NERD force field, atoms/sites within a molecule that do not interact by any other intramolecular potential are also allowed to interact through the Lennard-Jones potential.

For the polar group of the triglyceride, we turned to quantum mechanics to determine the necessary inter- and intramolecular parameters. The polar group of a triglyceride resembles a methyl acetate molecule. Our starting point for subsequent parametrization of the force field consisted of extensive quantum-chemical calculations for this molecule. Methyl acetate is a tractable molecule that can be studied fairly accurately at the quantum-mechanical level. Clearly, the functionality of methyl acetate is not exactly that encountered in the triglyceride, but it does contain the most relevant functional groups (see Figure 3). It is assumed that the interaction sites of a molecule are independent of each other and that the energy of the systems of interest can be parametrized in terms of a pairwise additive potential energy function.

2.1. Quantum Calculations. The equilibrium geometry of the model molecule, methyl acetate, was established by optimization with MP2/aug-cc-pVDZ using the Gaussian suite of programs.[26] The optimized geometry obtained was in good agreement with previously published results.[27] We next determined the intramolecular potentials due to bond stretching, bond bending, and torsions. It was assumed that, to a first approximation, all these interactions are uncoupled and can be calculated independently of each other. In such a case, a perturbation around the equilibrium distance or angle can be imposed in the geometry of the molecule, and a potential energy can be determined as a function of the degree of perturbation. For the bond stretching potential, each bond (excluding those between the hydrogens) was contracted and expanded 0.12 Å from its equilibrium distance in intervals of 0.02 Å. For the bond bending potential, each angle (also excluding those involving hydrogens) was varied ±12° from its equilibrium value in intervals of 2°. For the torsion potential, the torsion angle was incremented every 15° up to 180° from the equilibrium conformation (because of molecular symmetry, the remaining 180° can be mirrored from the ones calculated). A single-point energy calculation with MP2/aug-cc-pVDZ was performed for every perturbed geometry in order to construct each potential energy function.

For simplicity, the functional form of the NERD force field was used to parametrize the intramolecular potential for methyl acetate. Figure 4 shows each of the intramolecular potential functions fitted to eqs 4−6. Table 1 lists the force constants and Fourier coefficients of the regressed ab initio energies for each of the relevant intramolecular energy functions.

Intermolecular interactions require extensive energy calculations over the configurational space of a pair of molecules. Several recent studies have attempted to use "bare" intermolecular potentials from ab initio calculations to predict bulk properties without any empirical adjustment of the parameters.[28−31] That approach was not entirely possible in this work, and the information from ab initio interactions had to be refined in order to achieve quantitative agreement with experimental thermodynamic properties.

We initially calculated the ab initio interaction energy for several hundreds of configurations between a pair of methyl acetate molecules for a range of center-of-mass separations and relative orientations. A total of 610 configurations were considered, and for each of these, the intermolecular interaction energy was determined using the supermolecular approach.[32−35] In this method, three sets of calculations are required: one for the dimer, one with molecule A and the ghost of B, and another

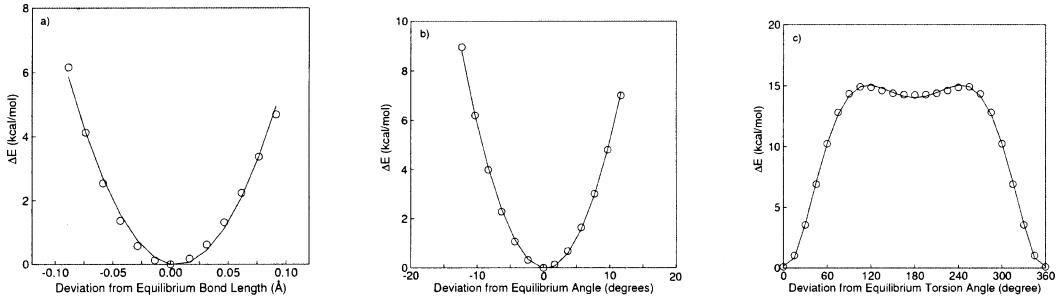

Figure 4. Sample intramolecular potentials for methyl acetate: (a) bond stretching; (b) bond bending; (c) torsional angle.

TABLE 1: Intramolecular Potential Parameters for Methyl Acetate Calculated from Quantum Chemical Calculations

	Bond Stretching—Eq 4	
	K_r, kJ/mol·Å^2	r_{eq}, Å
CH_3—O	2200	1.48
O—C	2700	1.40
C═O	3000	1.26
C—CH_3	2000	1.53
	Bond Bending—Eq 5	
	K_θ, kJ/mol·rad^2	θ_{eq}, deg
CH_3—O—C	923	117.0
O—C═O	1520	124.0
O—C—CH_3	1200	111.0
O═C—CH_3	1520	125.0
	Torsion Angle—Eq 6	
CH_3—O—C═O	$\phi_{eq} = 0.0$	$V_0 = 0.0$ kJ/mol
	$V_1 = 52.650$, $V_2 = 30.262$, $V_3 = 7.061$	
CH_3—O—C—CH_3	$\phi_{eq} = 180.0$	$V_0 = 0.0$ kJ/mol
	$V_1 = 52.074$, $V_2 = 33.679$, $V_3 = 6.493$	

with the ghost of A and molecule B. This inclusion of the ghost functions of molecules A and B is needed to correct for the well-known basis set superposition error (BSSE),[36,37] an unphysical lowering of the interaction energy due to the limited basis set used in the calculations. The interaction energy E_{AB}^{int} can be determined from

$$E_{AB}^{int} = E_{AB}\{AB\} - E_A\{AB\} - E_B\{AB\} \qquad (7)$$

where E_A is the energy of A and {AB} is the combined basis set of A and B. All the calculations were performed with MP2/cc-pVDZ, also using the Gaussian suite of programs. We also made use of a bond function located midway between the centers-of-mass of the molecules. This has been shown to improve the interaction energy description while adding only a small overhead to the computational load.[38,39] The monomer geometry was fixed at the equilibrium conformation.

Methyl acetate is a highly polar molecule; electrostatic interactions play a major part in its behavior. Electrostatic interactions can be included in the intermolecular potential through point charges q according to

$$U^{Coul} = \sum_{i<j} \frac{q_i q_j}{r_{ij}} \qquad (8)$$

The point charges are also calculated from quantum mechanics and determined from a fit of the electrostatic potential surface of methyl acetate with the same method and basis set (MP2/cc-pVDZ) used for the interaction energy calculations.

2.2. Parametrization of the Potential Energy Function. To make the methyl acetate and NERD force fields compatible with each other, we were restricted to a Lennard-Jones functional form and a Coulombic potential. A nonlinear least-squares fit was performed with the ab initio energies. During this procedure, the charges were fixed to the values obtained from the fit of the electrostatic potential surface. Each of the methyl groups was treated as a single interaction site (united-atom representation). An initial set of Lennard-Jones (ϵ and σ) parameters was obtained from this procedure, which were then tuned until good agreement was attained with the experimental condensed phase properties of methyl acetate.

TABLE 2: Intermolecular Potential Parameters for Methyl Acetate: See Eqs 2 and 8

site	ϵ, kJ/mol	σ, Å	q, a.u.
CH_3—	0.6347	3.830	0.200
—O—	0.6736	3.472	−0.400
—C—	0.7185	3.312	0.650
O═	0.7922	2.840	−0.500
—CH_3	0.6253	3.835	0.050

TABLE 3: Methyl Acetate Properties Calculated from *NPT* MD Simulations

	ρ, kg/m^3	ΔH, kJ/mol
this work	932(9)	33.5(20)
OPLS	897	30.1
experimental[40]	934	32.6

For the simulations of a condensed phase of methyl acetate, we used *NPT* molecular dynamics on a periodic box containing 80 molecules, with interactions spherically cut off at 10 Å. A reaction field correction was used for the long-range electrostatic interactions with the experimental value for the dielectric constant for methyl acetate ($\epsilon_{RF} = 6.97$[40]). The optimization of the Lennard-Jones parameters for methyl acetate was achieved by matching the density and heat of vaporization to experimental values at 25 °C and 1 bar. This required an iterative process, which quickly converged to a set of final values very similar to those determined from the original fit of the ab initio interaction energies. Table 2 provides the final set of Lennard-Jones parameters, and Table 3 gives the values of the calculated properties. Also included in the table are the properties calculated using the widely used OPLS force field.[21]

Another macroscopic property for validation of the resulting pair potential of methyl acetate was provided by the second virial coefficient, given by

$$B(T) = -\frac{1}{32\pi^3}\int_0^\infty r_{ij}^2\, dr_{ij} \int\int d\omega_i\, d\omega_j \left[\exp\left(\frac{-U_{ij}(r_{ij},\omega_i,\omega_j)}{k_B T}\right) - 1\right] \qquad (9)$$

Figure 5 shows the calculated and experimental second virial coefficients for methyl acetate, as well as those predicted using the OPLS potential.[21] The results of our calculations indicate the proposed model for methyl acetate describes reasonably well its macroscopic properties.

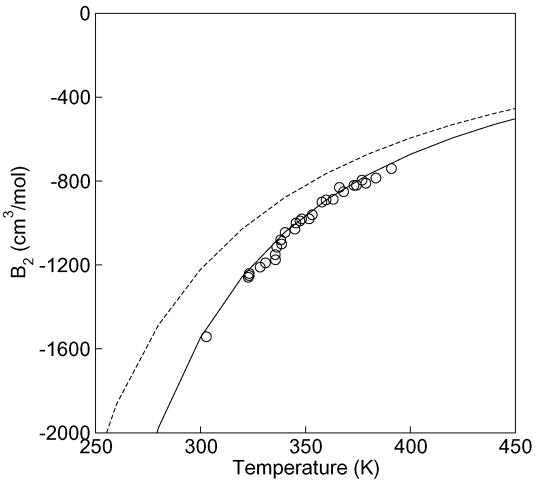

Figure 5. Second virial coefficient for methyl acetate: circles are experimental data,[54−56] the solid line is the results from our developed force field, and the dashed line is from the OPLS force field.[21]

TABLE 4: Predicted Properties for Selected Methyl Acetate Derivatives Using the Developed Force Field for Methyl Acetate and the NERD Force Field

compd	formula	ρ(calc/exp),[a] kg/m^3	ΔH(calc/exp),[a] kJ/mol
methyl pentanoate	$C_6H_{12}O_2$	886(9)/895	35.8/35.4
methyl laurate	$C_{13}H_{26}O_2$	870(7)/870	48.6/−
methyl palmitate	$C_{17}H_{34}O_2$	825(8)/825	52.2/−

[a] Reference 40.

Subsequent tests of the proposed model were conducted by examining the condensed phase properties of several methyl acetate derivatives that resemble a single chain of a triglyceride. Table 4 shows the results of our calculations and how they compare with available experimental data. Agreement with experiment is highly satisfactory. For these calculations, we simply combined the methyl acetate and NERD force fields. No further adjustments were made to any of the parameters. Note, however, that additional intramolecular parameters (stretching, bending, and torsion) for the group of atoms joining the methyl acetate and alkyl chain were necessary. These additional parameters are given in the Appendix.

The results obtained with the methyl acetate derivatives provide some assurance of the transferability of the developed force field to model triglycerides. For triglycerides, a few extra intramolecular parameters are required to account for the interactions along the glycerol part of the molecule. These parameters were also determined by quantum-chemical means, as described earlier; they are listed in the Appendix.

3. Triglyceride Properties

3.1. Simulation Details. The complete force field for triglycerides was used in molecular dynamics (MD) simulations. Both *NVT* and *NPT* calculations were performed using 40 molecules in a cubic box with periodic boundary conditions. Interactions were truncated and shifted at $r_c = 11$ Å with energies shifted at this distance. The systems evolved with a leapfrog integration algorithm[25] using a 2 fs time step. For static properties, data were averaged over 2 ns runs, and for transport properties, they were avaraged over at least 20 ns. To speed up some of the longer simulations, we also implemented a multiple time-step algorithm with a velocity−Verlet integration scheme.[41−44] Here, the short-time interactions (bond stretching and bond bending potentials) were propagated at 0.3 fs, and the long-time interactions (torsion and intermolecular potentials) at every 5 short time steps (long time step of 1.5 fs). This approach and combination of settings proved to speed up the calculations by approximately a factor of 5−10.

Simulations were performed for a range of temperatures from 273 to 373 K. Constant temperature and constant pressure simulations were maintained with the Berendsen's thermostat and barostat, respectively, by uniform scaling of the atomic velocities (temperature), and by uniform scaling of the atomic positions and box length (pressure). For all the calculations, a reaction-field correction was applied with continuum dielectric ϵ_{RF} to correct for long-range interactions due to electrostatics.[25] Whenever available, the known values of the dielectric constant were used;[40,45] otherwise, these were approximated on the basis of data for systems of similar chemical functionality.

The properties obtained from the simulations included density, heat of vaporization (where applicable for comparison), and viscosity. For viscosity calculations, the system was initially equilibrated at 1 bar and at the specified temperature for 1 ns. At that point, an *NVT* simulation was performed for at least 20 ns in order to accumulate the pressure tensor data to be used in the calculation of the viscosity. Long simulation runs were needed because the pressure cross-correlation function decays slowly. The atomic representation of the virial coefficient was adopted; sampling of the system was required at each time step (in the atomic representation of the virial coefficient, the pressure cross-correlation function oscillates at a high frequency related to the bond stretching potential—see Figure 6 for a typical

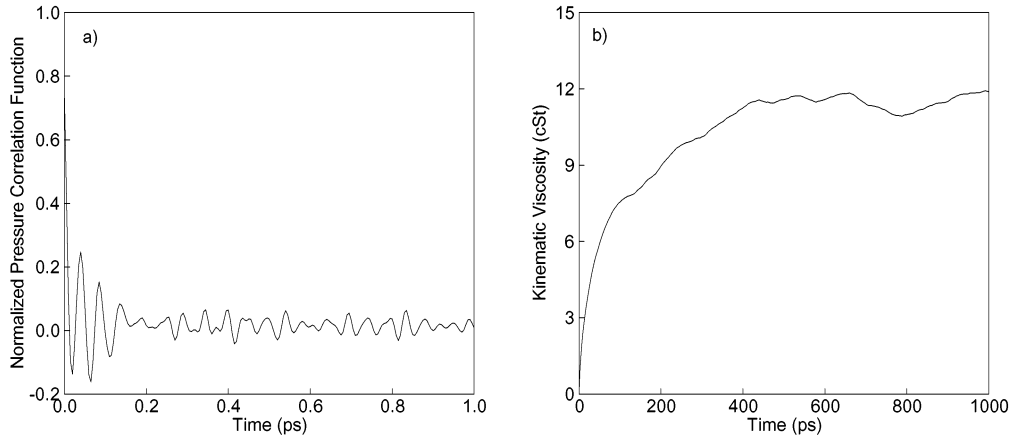

Figure 6. (a) Pressure cross-correlation function and (b) viscosity (integral of cross-correlation function) for triglycerides. The fluctuations in the pressure cross-correlation function come from the intramolecular (bond stretching and bending) interactions—atomic representation.

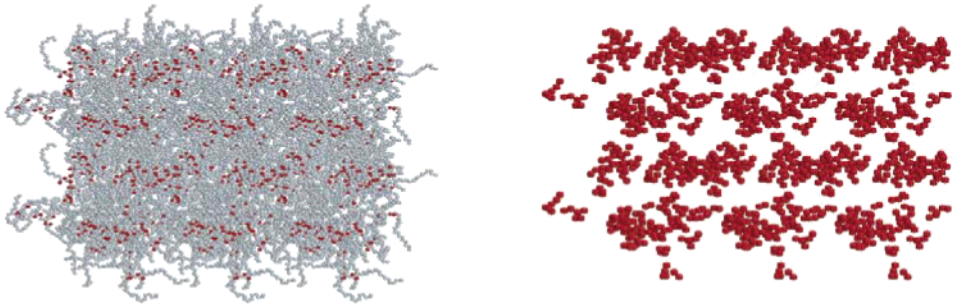

Figure 7. Evidence of formation of a layered structure in triglycerides. (a) Simulation box replicated three times in the horizontal direction and one time in the vertical direction. Light-colored atoms are carbons, and dark ones are the oxygens. (b) Only the oxygens are shown.

pressure cross-correlation function). After completion of the simulations, the shear viscosity (η) was calculated from[25,46]

$$\eta = \frac{V}{\rho k_B T}\int_0^\infty \langle P_{\alpha\beta}(t)\, P_{\alpha\beta}(0)\rangle \, dt \qquad (10)$$

where ρ, V, and T are the density, volume, and temperature of the system, respectively, k_B is the Boltzmann constant, and $P_{\alpha\beta}$ is the $\alpha\beta$ component of the symmetrized traceless portion of the stress tensor ($\sigma_{\alpha\beta}$), which is calculated from

$$P_{\alpha\beta} = \frac{\sigma_{\alpha\beta} + \sigma_{\beta\alpha}}{2} - \delta_{\alpha\beta}\left(\frac{1}{3}\sum_\gamma \sigma_{\gamma\gamma}\right) \qquad (11)$$

$$\sigma_{\alpha\beta}(t) = \frac{1}{N}[\sum_i v_\alpha^i(t)\, v_\beta^i(t) + \sum_{i<j} f_\alpha^{i,j}(t)(r_\beta^i(t) - r_\beta^j(t))] \qquad (12)$$

In eq 14, v_α^i and r_α^i are the α components of the velocity and position of atom i, $f_\alpha^{i,j}$ is the α component of the force on atom i due to atom j, and δ is the Kronecker delta function. Note that Mondello and Grest[46] have described a similar formulation for computing the viscosity by taking into account all the components of the pressure tensor,

$$\eta = \frac{V}{10\rho k_B T}\int_0^\infty \langle \sum_{\alpha\beta} P_{\alpha\beta}(t)\, P_{\alpha\beta}(0)\rangle \, dt \qquad (13)$$

We have used both formulations to calculate the viscosity from our simulations and determined that eq 13, the atomic representation of the virial coefficient, gives more consistent results (i.e., the integral of the pressure correlation function reached an asymptotic value faster).

3.2. Results and Discussion. Triglycerides are chemically similar to lipids in that they have long fatty acid chains (triglycerides have three compared to two for lipids). Lipids are know to self-assemble and form a layered structure; it is therefore of interest to determine if and to what extent triglycerides self-assemble in liquid phases. Note that experiments indicate that triglycerides form bilayer structures in the gel and solid states.[17] Our simulations reveal a pronounced tendency of the polar groups to aggregate and form structures resembling a bilayer. Figure 7 shows a snapshot of one of our simulations, with the periodic box replicated along two dimensions. This locally inhomogeneous structure suggests that it would be difficult for simple correlations developed for simple fluids to describe the thermodynamic and transport properties of triglyceride liquids.

Table 5 shows the predicted densities for several simple triglycerides obtained from *NPT* MD simulations at 1 bar. There is good agreement between calculated and experimental values.

TABLE 5: Predicted Liquid-Phase Properties for Simple Triglycerides

		density, kg/m^3		viscosity, cSt	
triglyceride[a]	T, °C	calc	exp[10,11,40,47−49 b]	calc	exp[10,11,40,47−49 b]
PrPrPr	20	1090	1099		
BuBuBu	20	1044	1035		
CaCaCa	20	1001	987		
LLL	80	918	882	9.6	8.3
	100	909	866	5.7	5.6
PPP	80	902	868	12.7	13.7
	100	890	854	10.9	8.8
SSS	80	895	862	13.6	16.5
	100	883	852	8.0	10.5
OOO-cis	40	923	901	76.3	38.6
	100	885	867	8.1	8.1
OOO-trans	40	925	901	41.7	38.6
	100	888	867	16.4	8.1
LiLiLi-cis	40	930		69.2	25.3
	100	894		22.2	5.4
LiLiLi-trans	40	928		66.9	25.3
	100	890		20.2	5.4
LeLeLe-cis	40	937		71.5	
	100	902		13.2	
LeLeLe-trans	40	931		50.6	
	100	897		7.5	

[a] PrPrPr, tripropanoin; BuBuBu, tributyrin; CaCaCa, tricaproin. [b] Note that experimental data for compounds with double bonds do not specify either cis or trans configuration.

The temperature dependence of the density is also fairly well described, although some minor differences are seen for a few triglycerides. Note that experimental data for pure triglycerides are limited; furthermore, available data are often of limited accuracy because of the difficulty associated with obtaining pure samples. For the triglycerides with double bonds, we considered both cis and trans configurations (for each configuration all chains were made either cis or trans). The conformation of the chains with bonds has a large impact on the properties of the triglyceride. For OOO, the cis configuration has a higher density than the trans form, whereas, for LiLiLi and LeLeLe, the trend is reversed (cis density is higher than trans density). These data suggest that the conformation of the chains plays an important role in the packing of these molecules in a condensed phase, which has great implication on the viscosities.

Table 5 also presents predicted viscosities for simple triglycerides and experimental data (or predictions from engineering correlations)[10,11,40,47,48,49] whenever available. Our molecular model for triglycerides appears to be accurate in predicting viscosity for these compounds. This is rewarding, particularly given the fact that only density data for small molecules were used to parametrize the force field. For the triglycerides with double bonds, the viscosity is strongly dependent on the conformation of the chains, that is, cis or trans. Excellent agreement with experimental data is obtained for the viscosity

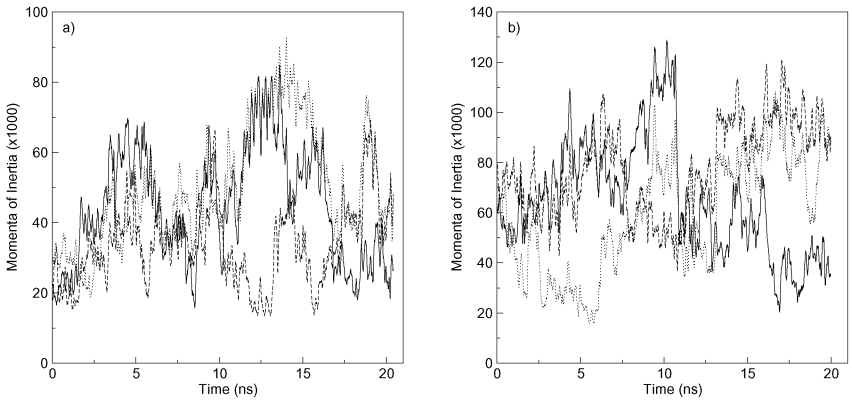

Figure 8. Principal moment of inertia for a molecule over the course of *NVT* MD simulations at $T = 100$ °C. (a) LiLiLi-cis and (b) LeLeLe-trans. The lines represent the different components of the moment of inertia: solid, I_{xx}; dashed, I_{yy}; dotted, I_{zz}.

of OOO-cis at 100 °C. Most sources of experimental data do not specify whether the double bonds of the alkyl chains are cis or trans; however, since the cis conformation is usually the predominant form for triglycerides, it is reassuring to find our predictions for OOO-cis to be in good agreement with available experimental data. The predictions for OOO at 40 °C are in better agreement with experiment for the trans conformation. Note, however, that the "experimental" viscosity is actually an extrapolated value from a correlation. For LiLiLi, there is a significant discrepancy between the predicted values and experimental data at both 40 and 100 °C. It must be again noted that the form and purity of the triglyceride sample were not reported for the experimental measurement. To the best of our knowledge, experimental data for LeLeLe are not available.

Among the triglycerides with double bonds, the cis and trans conformations have different impacts on the viscosity, not obvious at first sight. If we compare the results at 100 °C, the trans conformation for OOO has a higher viscosity than the cis one, whereas, for LiLiLi and LeLeLe, the cis conformation viscosity is higher. This behavior can be understood by the density of the triglycerides: the density of the cis form of LiLiLi and LeLeLe is higher than that of the trans conformation. The density, and in turn the viscosity, are higher for the cis conformation because, in the cis form, the alkyl chains are able to coil and assume a more compact form. We have quantified this change in the structure of the molecules by measuring the average distance between the carbonyl carbon and the last carbon of all alkyl chains; we find that, at 100 °C, these distances are 13.91, 12.66, and 11.92 Å for the cis forms of OOO, LiLiLi, and LeLeLe, respectively.

Viscosity calculations for these triglycerides require long simulation runs (tens of nanoseconds), capable of capturing the conformational fluctuations of the molecules. Figure 8 shows the principal components of the moment of inertia for a molecule from each of the LiLiLi-cis and LeLeLe-trans systems. The components of the moment of inertia provide a measure of the molecular shape; we see large fluctuations over the course of the simulations. For example, for the molecule considered in Figure 8a, the I_{zz} component (dotted line) steadily increases by about a factor of 4 over 15 ns.

We now consider mixtures of triglycerides comprising as many as 10 components, and pure triglycerides containing more than one type of fatty acid chain. Experimental data are available for vegetable oils and butter products; unfortunately, complete descriptions of their composition in terms of different triglycerides are seldom available. Oftentimes the reported composition only provides the amount of the various fatty acids that constitute the triglycerides (this information only is not sufficient to determine which triglycerides are present in the mixture).

TABLE 6: Triglyceride Composition for Canola Oil[50] and Cocoa Butter[51]

canola oil			cocoa butter		
	mole fraction			mole fraction	
	actual	model		actual	model
POP	0.0090		PPS	0.006	
PLiP	0.0057		PSS	0.023	
POO	0.0909	0.100	POP	0.158	0.200
POLi	0.0668	0.075	POS	0.401	0.475
POLe	0.0390		SOS	0.275	0.325
PLiLe	0.0105		POO	0.027	
SOO	0.0214		PLiP	0.016	
OOO	0.2376	0.275	PLiS	0.023	
OOLi	0.2409	0.275	SOO	0.026	
OOLe	0.1776	0.200	SLiS	0.022	
OLiLe	0.0756	0.075	SLiO	0.007	
OLeLe	0.0249		OOO	0.004	
			SOA	0.011	

TABLE 7: Liquid Density for Triglyceride Mixtures

mixture	T, °C	density, kg/m^3
canola oil	27	917
	87	881
cocoa butter	57	893
	157	832

Table 6 provides the compositions of the two mixtures considered in this work, canola oil[50] and cocoa butter.[51] The normalized composition used in the simulations is also given in that table; these are complex mixtures, and in the interest of simplicity, we have chosen to include in our simulations only those components present in significant amounts; our model canola oil and cocoa butter contain six and three triglycerides, respectively. Figure 9 shows the predicted viscosity for canola oil and cocoa butter and the corresponding experimental viscosities. Our predictions provide an accurate description of the viscosities of these mixtures and their temperature dependence. We note again that these results represent complete predictions. The densities of canola oil and cocoa butter are listed in Table 7 (experimental data are not available).

Table 8 shows the predicted properties of two mixed triglycerides denoted by AP-75 and AP-85.[52] These two oils, which are commercial lubricants marketed by Cargill Inc., have been formulated from vegetable oils. The exact composition of these oils is proprietary; here we merely point out that in our simulations AP-75 and AP-85 consisted of a mixture of five and four mixed triglycerides, respectively (AP75 has a mid-oleic fraction, whereas AP-85 has a high-oleic fraction). The

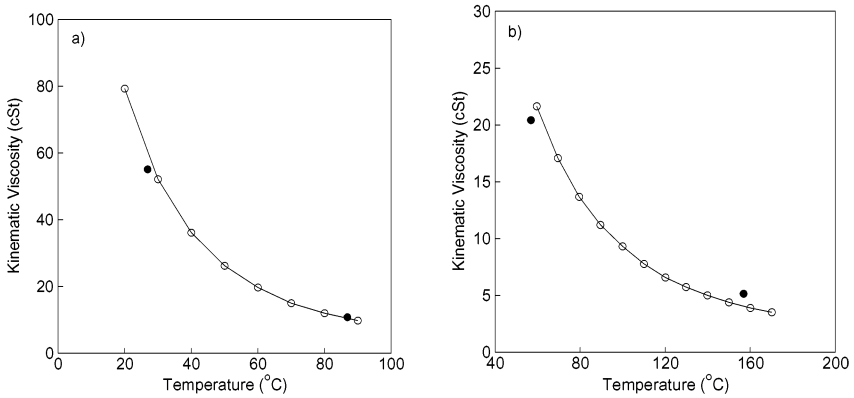

Figure 9. Kinematic viscosity for (a) canola oil and (b) cocoa butter. Open symbols are experimental data,[50,51] and filled circles are predicted viscosities from simulations.

TABLE 8: Predicted Properties for AP Oil Mixtures

		density, kg/m^3		viscosity, cSt		viscosity index	
	T, °C	calc	exp[a]	calc	exp[a]	calc	exp
AP-75	40	909	903	36.2	38.9	174	156
	100	872		10.6	8.42		
AP-85	40	909	903	35.9	39.9	165	156
	100	872		8.7	8.59		

[a] Reference 52.

predicted densities and viscosities of the AP oils compare favorably with measured values at both 40 and 100 °C. The temperature dependence is of great importance here because it is widely used for industrial characterization of lubricants with the so-called viscosity index (VI) (ASTM D-2270[53]). This parameters is also well predicted from our results.

Having established that the proposed force field is appropriate for simulations of triglycerides, we can now investigate some of the physical consequences of simple modifications to these molecules. As mentioned in the Introduction, triglycerides are sought for lubrication applications with environmentally benign, biodegradable products. To improve and design the properties of triglycerides to meet certain lubrication specifications, it is desirable to know how the structural functionality of these molecules influences their transport properties. For example, it is of interest to know the effect of adding small alkyl groups to the main chains of the triglyceride, and how transport properties change with the length and position of the added groups. Similar questions arise regarding the number and position of double bonds along the main chains, as well as the placement of heteroatoms.

Within this context, we investigated how the viscosity is affected by changes in the molecular structure of triglycerides. One functionality identified among the systems studied is the number of double bonds per chain. The compounds of interest here all have 18 carbons per chain, and they are SSS (no double bonds), OOO (one double bond at position 9), LiLiLi (two double bonds at positions 9 and 12), and LeLeLe (three double bonds at positions 9, 12, and 15)—the numbering starts at the carbonyl carbon of each chain. Figure 10 shows a plot comparing the changes in the viscosity among these compounds at 100 °C. We see that viscosity increases in proportion to the number of double bonds per chain (from SSS to LiLiLi). Considering either the cis or trans conformation, this behavior can be understood by the conformational changes imposed by double bonds, which cause a increase in the density. The increase in viscosity between the cis forms of OOO and LiLiLi is much more pronounced for the trans form, and here the reasoning is due to the more compact structure by the coiling

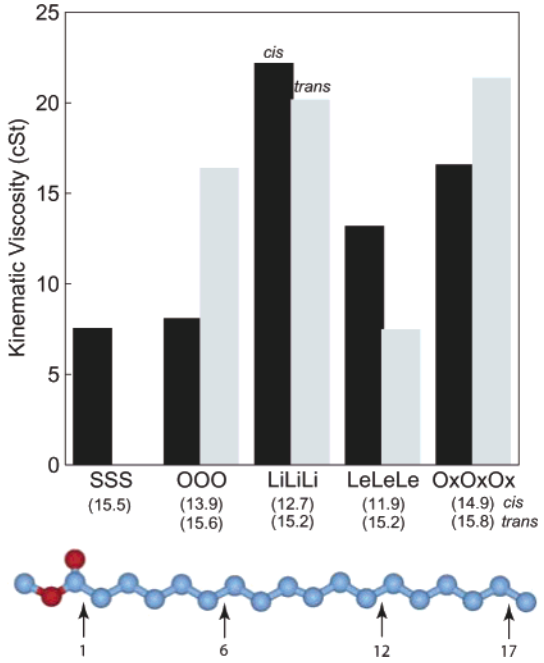

Figure 10. Effect of number and position of the double bonds on triglycerides. Viscosities calculated at $T = 100$ °C. The number in parentheses below the label indicates the average distance (in Å) between the carbonyl carbon and the last carbon in the chain. A single chain for a TAG molecule is shown with the numbering scheme for the double bonds. The positions of the double bonds for the TAGs listed in the graphs are as follows: SSS has no double bond; OOO one at position 9; LiLiLi two at positions 9 and 11; LeLeLe three at positions 9, 11, and 13; OxOxOx one at position 3.

of the chains, thereby resulting in more entanglements and a greater resistance to flow. This can also be seen from the average distance between the carbonyl carbon and the last carbon of all alkyl chains; for the trans conformations there is only a small decrease in the average end-distance (about 0.4 Å), whereas, for the cis case, the change is more substantial (about 1.2 Å), resulting from the coiling of the chains.

For the triglyceride with three double bonds (LeLeLe), the viscosity decreases significantly compared to the case of LiLiLi and the argument given previously does not hold. In this case, the density of LeLeLe, both cis and trans conformations, is higher than that for LiLiLi; therefore, even though the packing of the molecules is more compact, there are other rheological effects in play. For the cis conformation, the three double bonds make the structure of the molecules much more compact (more closed, like a sphere), which in turn is less prone to entangle with other chains, thus the lower viscosity but higher density.

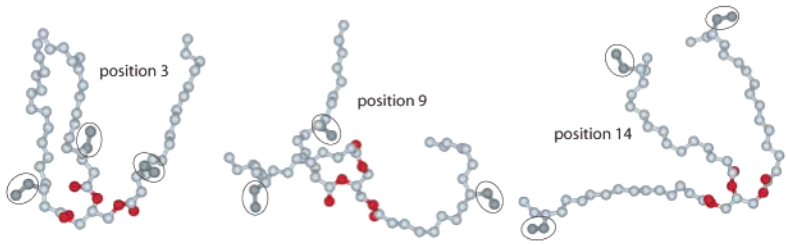

Figure 11. Model triglyceride molecules with an ethyl group added to each chain.

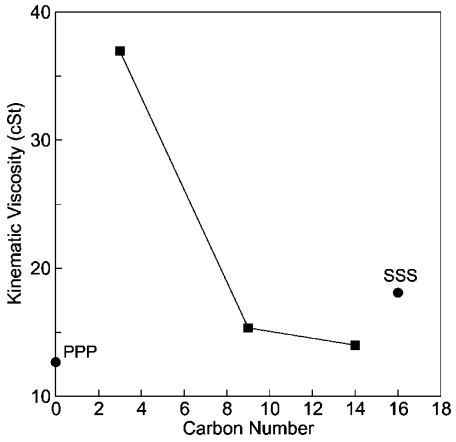

Figure 12. Effect of adding an ethyl group to each chain of a PPP molecule. Viscosities calculated at $T = 80$ °C. The circles are the viscosities of the unmodified PPP and SSS. The squares represent the viscosities for the modified triglycerides.

We have also considered how the position of the double bond affects the viscosity of the system. The last entry in Figure 10 shows the results for a hypothetical compound (OxOxOx) containing one double bond per chain, same as OOO, but placed at position 3 (closer to the polar backbone). This change in the structure of the triglyceride results in a significant increase in the viscosity; by making the chain stiffer near the polar part of the triglyceride, the structure becomes more open and the viscosity is higher. For this hypothetical compound, the cis and trans forms have identical densities of 887 kg/m^3 at 100 °C. As before, the average distance between the carbonyl carbon and the last carbon was calculated for this hypothetical compound and found to be greater than that for OOO.

The effect of adding an ethyl group to each of the chains of a PPP molecule is considered in Figure 11. Results are presented for three molecules: an ethyl group located at (a) position 3 (near the polar group), (b) position 9 (the middle of the chain), and (c) position 14 (near the end of the chain). The viscosity for each of these cases is illustrated in Figure 12. The figure also includes the viscosities of PPP (no ethyl group added) and SSS (one ethyl group added to the last carbon of PPP), provided as a reference for comparison. Here we see that, by placing the ethyl group near the polar backbone, the viscosity is dramatically increased, about three times higher than the viscosity of PPP. As the ethyl group is positioned farther away down the chain, the viscosity decreases and approaches that of SSS. It is also interesting to note that the viscosity for the case with the ethyl group at position 14 is somewhat lower than the viscosity of SSS, suggesting that there is not a simple linear correlation between the number of carbons per chain and structure. In analogy to our observations regarding the position of the double bonds, the effects related to the location of the ethyl group can be understood on the basis of the molecular conformation of the molecules. With the ethyl group near the polar backbone, stearic hindrance leads to a more open structure (the average distance between the carbonyl carbon and the last carbon is 14.4 Å for the ethyl group at position 3 compared to 14.2 Å for PPP). As the ethyl group is placed farther away from the polar backbone, its effect on the conformation of the molecule and the ensuing viscosity decreases (the average end chain distance is 13.5 and 14.1 Å for positions 9 and 14, respectively).

TABLE 9: Complete Force Field Parameters for Triacylglycerols

Bond Stretching—Eq 4

	K_r, kJ/mol·Å^2	r_{eq}, Å
C1−O2	2200	1.48
O2−C3	2700	1.40
C3−O4	3000	1.26
C3−C5	2000	1.53
C5−C6	802.3	1.54
C1−C1	2000	1.60

Bond Bending—Eq 5

	K_θ, kJ/mol·rad^2	θ_{eq}, deg
C1−O2−C3	923	117.0
O2−C3−O4	1520	124.0
O2−C3−C5	1200	111.0
O4−C3−C5	1520	125.0
C3−C5−C6	864	114.0
O2−C1−C1	1000	109.0
C1−C1−C1	1200	119.0

Torsion Angle—Eq 6

	ϕ_{eq}	V_0	V_1	V_2	V_3
C1−O2−C3−O4	0.0	0.0	52.650	30.262	7.061
C1−O2−C3−C5	180.0	0.0	52.074	33.679	6.493
O2−C3−C5−C6	180.0	0.0	3.076	1.459	2.928
O4−C3−C5−C6	0.0	0.0	3.076	1.459	2.928
C3−C5−C6−C7	180.0	0.0	51.596	−44.053	32.759
C1−C1−O2−C3	180.0	0.0	32.302	−15.707	26.392
C1−C1−C1−O2	180.0	0.0	8.608	42.768	20.228
O2−C1−C1−O2	180.0	0.0	8.608	42.768	20.228
C═C−C−C	180.0	0.0	0.130	−1.837	−8.687
C−C═C−C	180.0	0.0	47.853	264.781	15.129

4. Conclusions

In this study, we have shown how computational tools can be successfully used to predict physical properties of large and complex molecules such as triglycerides. An accurate force field was developed to model the entire molecule by combining the NERD force field and a potential model for methyl acetate. The NERD force field was used to describe the aliphatic chains of triglycerides, whereas the polar part was accounted for by a new potential developed from quantum-chemical calculations of the intra- and intermolecular interactions of methyl acetate. This approach led to a complete description for triglycerides, which was also tested with selected methyl acetate derivatives. The developed molecular model was used with molecular dynamics simulations to predict the properties for a number of simple and mixed triglycerides. Calculated densities and viscosities were in good agreement with available measured values, showing that our model was accurate and reliable to study

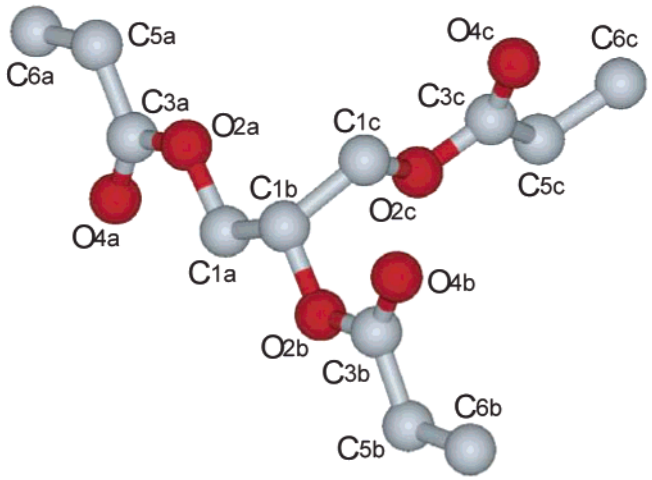

Figure 13. Sample triacylglycerol molecule with the numbering convention used to described the parameters shown in Table 9.

triglycerides. We also investigated some structure−property relationships in order to obtain a clear understanding of how structural changes affect the viscosity of these compounds. We discussed the effect of the number and position of double bonds along each chain of triglycerides, as well as the addition of an ethyl group as a branch from the main chain. From the results, we conclude that the viscosity can be significantly changed by modifying the stiffness of the chains of the triglycerides. This systematic study of structure−property relationships will develop a means to study the molecular architecture of compounds tuned to specific properties to help in the development of new products. Moreover, this method proves to be a flexible and inexpensive tool requiring minimum input.

Acknowledgment. We are very grateful for the financial support to this project by Cargill Inc. MJB was supported by a Computational Science Graduate Fellowship (DE-FG02-97ER25308) funded by the DOE through the Krell Institute. Partial support of this work from the NSF is also gratefully acknowledged.

Appendix

The complete list of parameters for the developed molecular model for triacylglycerols shown in Table 9 follows the numbering convention for the atoms/sites shown in Figure 13.

References and Notes

(1) Zaher, F. A.; Nomany, H. M. *Grasas Aceites* **1988**, *49*, 235.
(2) Erhan, S. Z.; Asadauskas, S. *Ind. Crops Prod.* **2000**, *11*, 277.
(3) Willing, A. *Chemosphere* **2001**, *43*, 89.
(4) Pirro, D. M.; Wessol, A. A. Environmental Lubricants. In , 2nd ed.; Marcel Dekker: New York, 2001; pp 105−118.
(5) Hörner, D. *J. Synth. Lubr.* **2002**, *18*, 327.
(6) Kodali, D. R. *Ind. Lubr. Tribol.* **2002**, *54*, 165.
(7) Choi, U. S.; Ahn, B. G.; Kwon, O. K.; Chun, Y. J. *Tribol. Int.* **1997**, *30*, 667.
(8) Bírová, A.; Pavlovičová, A.; Cvengroš, J. *J. Synth. Lubr.* **2002**, *18*, 291.
(9) Asadauskas, S.; Perez, J. M.; Duda, J. L. *J. Soc. Tribol. Lubr. Eng.* **1997**, 35.
(10) Bockisch, M. *Fats and Oils Handbook*; AOCS Press: Champaign, IL, 1998.
(11) Gunstone, F. D., Harwood, J. L., Padley, F. B., Eds. *The Lipid Handbook*; Chapman and Hall: New York, 1986.
(12) Hagemann, J. W.; Rothfus, J. A. *J. Am. Oil Chem. Soc.* **1983**, *60*, 1308.
(13) Hagemann, J. W.; Rothfus, J. A. *J. Am. Oil Chem. Soc.* **1988**, *65*, 1493.
(14) Hagemann, J. W.; Rothfus, J. A. *J. Am. Oil Chem. Soc.* **1992**, *69*, 429.
(15) Hagemann, J. W.; Rothfus, J. A. *J. Am. Oil Chem. Soc.* **1993**, *70*, 211.
(16) Yan, X.-Y.; Huhn, S. D.; Klemann, L. P.; Otterburn, M. S. *J. Agric. Food Chem.* **1994**, *42*, 447.
(17) Engelsen, S. B.; Brady, J. W.; Sherbon, J. W. *J. Agric. Food Chem.* **1994**, *42*, 2099.
(18) Brooks, B. R.; Bruccoleri, R. E.; Olafson, B. D.; States, D. J.; Swaminathan, S.; Karplus, M. *J. Comput. Chem.* **1983**, *4*, 187.
(19) Cornell, W. D.; Cieplak, P.; Bayly, C. I.; Gould, I. R.; Merz, K. M.; Ferguson, D. M.; Spellmeyer, D. C.; Fox, T.; Caldwell, J. W.; Kollman, P. A. *J. Am. Chem. Soc.* **1995**, *117*, 5179.
(20) Cornell, W. D.; Cieplak, P.; Bayly, C. I.; Gould, I. R.; Merz, K. M.; Ferguson, D. M.; Spellmeyer, D. C.; Fox, T.; Caldwell, J. W.; Kollman, P. A. *J. Am. Chem. Soc.* **1996**, *118*, 2309.
(21) Briggs, J. M.; Nguyen, T. B.; Jorgensen, W. L. *J. Phys. Chem.* **1991**, *95*, 3315.
(22) Nath, S. K.; Escobedo, F. A.; de Pablo, J. J. *J. Chem. Phys.* **1998**, *108*, 9905.
(23) Nath, S. K.; de Pablo, J. J. *Mol. Phys.* **2000**, *98* (4), 231.
(24) Nath, S. K.; Banaszak, B. J.; de Pablo, J. J. *J. Chem. Phys.* **2001**, *114*, 3612.
(25) Allen, M. P.; Tidesley, D. J. *Computer Simulation of Liquid*; Oxford University Press: New York, 1987.
(26) Frisch, M. J.; Trucks, G. W.; Schlegel, H. B.; Scuseria, G. E.; Robb, M. A.; Cheeseman, J. R.; Zakrzewski, V. G.; Montgomery, J. A.; Stratmann, R. E.; Burant, J. C.; Dapprich, S.; Millam, J. M.; Daniels, A. D.; Kudin, K. N.; Strain, M. C.; Farkas, O.; Tomasi, J.; Barone, V.; Cossi, M.; Cammi, R.; Mennucci, B.; Pomelli, C.; Adamo, C.; Clifford, S.; Ochterski, J.; Petersson, G. A.; Ayala, P. Y.; Cui, Q.; Morokuma, K.; Malick, D. K.; Rabuck, A. D.; Raghavachari, K.; Foresman, J. B.; Cioslowski, J.; Ortiz, J. V.; Stefanov, B. B.; Liu, G.; Liashenko, A.; Piskorz, P.; Komaromi, I.; Gomperts, R.; Martin, R. L.; Fox, D. J.; Keith, T.; Al-Laham, M. A.; Peng, C. Y.; Nanayakkara, A.; Gonzalez, C.; Challacombe, M.; Gill, P. M. W.; Johnson, B. G.; Chen, W.; Wong, M. W.; Andres, J. L.; Head-Gordon, M.; Replogle, E. S.; Pople, J. A. *Gaussian 98*; Gaussian Inc.: 1998.
(27) Pyckhout, W.; van Alsenoy, C.; Geise, H. J. *J. Mol. Struct.* **1986**, *144*, 265.
(28) Sum, A. K.; Sandler, S. I. *Mol. Phys.* **2002**, *100*, 2433.
(29) Sum, A. K.; Sandler, S. I.; Bukowski, R.; Szalewicz, K. *J. Chem. Phys.* **2002**, *116*, 7627.
(30) Sum, A. K.; Sandler, S. I.; Bukowski, R.; Szalewicz, K. *J. Chem. Phys.* **2002**, *116*, 7637.
(31) Naicker, P. K.; Sum, A. K.; Sandler, S. I. *J. Chem. Phys.* **2003**, *118*, 4086.
(32) Chałasiński, G.; Szczęśniak, M. M. *Mol. Phys.* **1988**, *63*, 205.
(33) Chałasiński, G.; Szczęśniak, M. M. *Chem. Rev.* **1994**, *94*, 1723.
(34) Chałasiński, G.; Szczęśniak, M. M. *Chem. Rev.* **2000**, *100*, 4227.
(35) Engkvist, O.; Astrand, P. O.; Karlstrom, G. *Chem. Rev.* **2000**, *100*, 4087.
(36) van Duijneveldt, F. B.; van Duijneveldt-van de Rijdt, J. G. C. M.; van Lenthe, J. H. *Chem. Rev.* **1994**, *94*, 1873.
(37) Kestner, N. R.; Combariza, J. E. In *Rev. Comput. Chem.*; Lipkowitz, K. B., Boyd, D. B., Eds.; Wiley-VHC: New York, 1999; Vol. 13, pp 99−132.
(38) Williams, H. L.; Mas, E. M.; Szalewicz, K.; Jeziorski, B. *J. Chem. Phys.* **1995**, *103*, 7374.
(39) Torheyden, M.; Jansen, G. *Theor. Chem. Acc.* **2000**, *104*, 370.
(40) Lide, D. R., Ed. *CRC Handbook of Chemistry and Physics*, 76th ed.; CRC: Boca Raton, FL, 1995.
(41) Procacci, P.; Marchi, M. Multiple time steps algorithms for the atomistic simulations of complex molecular systems. In NATO ASI C545; Kluwer: Dordrecht, Germany, 2000; pp 333−387.
(42) Marchi, M.; Procacci, P. *J. Chem. Phys.* **1999**, *109*, 5194.
(43) Watanabe, M.; Karplus, M. *J. Chem. Phys.* **1993**, *99*, 8063.
(44) Watanabe, M.; Karplus, M. *J. Phys. Chem.* **1995**, *99*, 5680.
(45) Gouw, T. H.; Vlugter, J. C. *Fette Seifen Anstrichm.* **1967**, *69*, 223.
(46) Mondello, M.; Grest, G. S. *J. Chem. Phys.* **1997**, *106*, 9327.
(47) Kishore, K.; Shobha, H. K.; Mattamal, G. J. *J. Phys. Chem.* **1990**, *94*, 1642.
(48) Phillips, J. C.; Mattamal, G. J. *J. Chem. Eng. Data* **1978**, *23*, 1.
(49) Phipps, L. W. *Nature* **1962**, *193*, 541.
(50) Rabelo, J.; Batista, E.; Cavaleri, F. W.; Meirelles, A. J. A. *J. Am. Oil Chem. Soc.* **2000**, *77*, 1255.
(51) Azian, M. N.; Kamal, A. A. M.; Panau, F.; Ten, W. K. *J. Am. Oil Chem. Soc.* **2001**, *78*, 1001.
(52) Oils, C. I.; Lubricants. http://www.techoils.cargill.com/products/canola.htm.
(53) *Annual Book of ASTM Standards, D 2270-93*, 1993.
(54) Dymond, J. H.; Smith, E. B. *The Virial Coefficients of Gases*; Clarendon: Oxford, U.K., 1969.
(55) McElroy, P. J.; Gellen, A. T.; Kolahi, S. S. *J. Chem. Eng. Data* **1990**, *35*, 38.
(56) McElroy, P. J.; Robertson, G. A.; Kolahi, S. S. *J. Chem. Eng. Data* **1990**, *35*, 427.